Research Article | Vol. 25, No. 14 | 10 Jul 2017 | OPTICS EXPRESS 16274
Optics EXPRESS

Photonics-based broadband radar for high-resolution and real-time inverse synthetic aperture imaging

FANGZHENG ZHANG,[1] QINGSHUI GUO,[1] ZIQIAN WANG,[2] PEI ZHOU,[1] GUOQIANG ZHANG,[2] JUN SUN,[2] AND SHILONG PAN[1,*]

[1]*Key Laboratory of Radar Imaging and Microwave Photonics, Ministry of Education, Nanjing University of Aeronautics and Astronautics, Nanjing 210016, China*
[2]*Key Laboratory for Intellisensing, Nanjing Research Institute of Electronics Technology, Nanjing, 210039, China*
**pans@ieee.org*

Abstract: A photonics-based radar with generation and de-chirp processing of broadband linear frequency modulated continuous-wave (LFMCW) signal in optical domain is proposed for high-resolution and real-time inverse synthetic aperture radar (ISAR) imaging. In the proposed system, a broadband LFMCW signal is generated by a photonic frequency quadrupler based on a single integrated electro-optical modulator, and the echoes reflected from the targets are de-chirped to a low frequency signal by a microwave photonic frequency mixer. The proposed radar can operate at a high frequency with a large bandwidth, and thus achieve an ultra-high range resolution for ISAR imaging. Thanks to the wideband photonic de-chirp technique, the radar receiver could apply low-speed analog-to-digital conversion and mature digital signal processing, which makes real-time ISAR imaging possible. A K-band photonics-based radar with an instantaneous bandwidth of 8 GHz (18-26 GHz) is established and its performance for ISAR imaging is experimentally investigated. Results show that a recorded two-dimensional imaging resolution of ~2 cm × ~2 cm is achieved with a sampling rate of 100 MSa/s in the receiver. Besides, fast ISAR imaging with 100 frames per second is verified. The proposed radar is an effective solution to overcome the limitations on operation bandwidth and processing speed of current radar imaging technologies, which may enable applications where high-resolution and real-time radar imaging is required.

OCIS codes: (060.5625) Radio frequency photonics; (350.4010) Microwaves; (280.6730) Synthetic aperture radar; (280.4750) Optical processing of radar images.

References and links

1. P. Almorox-Gonzalez, J. T. González-Partida, M. Burgos-García, C. D. L. Morena-Alvarez-Palencia, L. Arche-Andradas, and B. P. Dorta-Naranjo, "Portable high resolution LFM-CW radar sensor in millimeter-wave band," in *Proc. 2007 Int. Conf. Sensor Technologies Applications* (2007).
2. J. Ping, A. Ling, T. Quan, and C. Dat, "Generic unmanned aerial vehicle (UAV) for civilian application," in *I Proc. Conference on Sustainable utilization and Development in Engineering and Technology* (2012), pp. 289–294.
3. B. Valdes, Y. Alvarze, S. Mantzavinos, C. M. Rappaport, F. Las-Heras, and J. A. Martinez-Lorenzo, "Improving security screening: a comparison of multistatic radar configurations for human body imaging," IEEE Antennas Propag. Mag. **58**(4), 35–47 (2016).
4. V. C. Chen and M. Martorella, *Inverse Synthetic Aperture Radar Imaging: Principles, Algorithms and Applications* (SciTech Publishing, 2014).
5. O. Caner, *Inverse Synthetic Aperture Radar Imaging with MATLAB Algorithms* (John Wiley & Sons, 2012).
6. D. A. Robertson, D. G. Macfarlane, R. I. Hunter, C. L. Cassidy, N. Liombart, E. Candini, T. Bryllert, M. Ferndahl, H. Lindstrom, J. Tenhunen, H. Vasama, J. Huopana, T. Selkala, and A. J. Vuotikka, "High resolution, wide field of view, real time 340GHz 3D imaging radar for security screening," in *Proc. SPIE Passive and Active Millimeter-Wave Imaging* (2017), paper 101890C.
7. B. B. Cheng, G. Jing, C. Wang, C. Yang, Y. W. Cai, Q. Chen, X. Huang, G. H. Zeng, J. Jiang, X. J. Deng, and J. Zhang, "Real-time imaging with a 140 GHz inverse synthetic aperture radar," IEEE Trans. THz Sci. Technol. **3**(5), 606–616 (2013).

#296748 https://doi.org/10.1364/OE.25.016274
Journal © 2017 Received 29 May 2017; revised 26 Jun 2017; accepted 27 Jun 2017; published 29 Jun 2017

Optics EXPRESS

8. Q. Li, D. Yang, X. H. Mu, and Q. L. Huo, "Design of the L-band wideband LFM signal generator based on DDS and frequency multiplication," in *International Conference on Microwave and Millimeter Wave Technology* (ICMMT, 2012).
9. B. Zhang, Y. M. Pi, and J. Li, "Terahertz imaging radar with inverse aperture synthesis techniques: system structure, signal processing, and experiment results," IEEE Sens. J. **15**(1), 290–299 (2015).
10. P. Ghelfi, F. Laghezza, F. Scotti, G. Serafino, S. Pinna, D. Onori, E. Lazzeri, and A. Bogoni, "Photonics in radar systems," IEEE Microw. Mag. **16**(8), 74–83 (2015).
11. J. Capmany and D. Novak, "Microwave photonics combines two worlds," Nat. Photonics **1**(6), 319–330 (2007).
12. J. Yao, "Microwave photonics," J. Lightwave Technol. **27**(3), 314–335 (2009).
13. S. L. Pan, D. Zhu, S. F. Liu, K. Xu, Y. T. Dai, T. L. Wang, J. G. Liu, N. H. Zhu, Y. Xue, and N. J. Liu, "Satellite payloads pay off," IEEE Microw. Mag. **16**(8), 61–73 (2015).
14. H. Gao, C. Lei, M. Chen, F. Xing, H. Chen, and S. Xie, "A simple photonic generation of linearly chirped microwave pulse with large time-bandwidth product and high compression ratio," Opt. Express **21**(20), 23107–23115 (2013).
15. W. Li and J. P. Yao, "Generation of linearly chirped microwave waveform with an increased time-bandwidth product based on a tunable optoelectronic oscillator," J. Lightwave Technol. **32**(20), 3573–3579 (2014).
16. P. Zhou, F. Zhang, Q. Guo, and S. Pan, "Linearly chirped microwave waveform generation with large time-bandwidth product by optically injected semiconductor laser," Opt. Express **24**(16), 18460–18467 (2016).
17. H. Zhang, W. Zou, and J. Chen, "Generation of a widely tunable linearly chirped microwave waveform based on spectral filtering and unbalanced dispersion," Opt. Lett. **40**(6), 1085–1088 (2015).
18. P. Ghelfi, F. Laghezza, F. Scotti, G. Serafino, A. Capria, S. Pinna, D. Onori, C. Porzi, M. Scaffardi, A. Malacarne, V. Vercesi, E. Lazzeri, F. Berizzi, and A. Bogoni, "A fully photonics-based coherent radar system," Nature **507**(7492), 341–345 (2014).
19. S. J. Strutz and K. J. Williams, "An 8–18-GHz all-optical microwave downconverter with channelization," IEEE Trans. Microw. Theory Tech. **49**(10), 1992–1995 (2001).
20. V. R. Pagán, B. M. Haas, and T. E. Murphy, "Linearized electrooptic microwave downconversion using phase modulation and optical filtering," Opt. Express **19**(2), 883–895 (2011).
21. E. H. W. Chan and R. A. Minasian, "Microwave photonic downconverter with high conversion efficiency," J. Lightwave Technol. **30**(23), 3580–3585 (2012).
22. C. Lin, P. Shih, J. Chen, W. Xue, P. Peng, and S. Chi, "Optical millimeter-wave signal generation using frequency quadrupling technique and no optical filtering," IEEE Photonics Technol. Lett. **20**(12), 1027–1029 (2008).

1. Introduction

In order to identify, classify targets efficiently, and then take actions timely, high-resolution and real-time radar imaging is highly desired in many applications, such as pilotless automobiles, unmanned aerial vehicles and quick security checks [1–3]. Inverse synthetic aperture radar (ISAR) has been widely employed for target imaging, which uses signal processing technique rather than large aperture antennas to identify a moving target [4, 5]. To realize high-resolution and real-time ISAR imaging, detecting signals with a very large bandwidth, as well as fast digital signal processing are indispensable [6]. Through electronic de-chirping of linear frequency modulated continuous-wave (LFMCW) signals, fast or even real-time imaging can be achieved [7]. However, due to the limited bandwidth of the state-of-the-art electronic devices, e.g., direct generation of linear frequency modulation (LFM) signal by means of a direct digital synthesizer (DDS) is limited to a few gigahertz [8], it's difficult to achieve a high imaging resolution. One possible solution is to increase the carrier frequency to get a larger bandwidth. For example, a THz ISAR system with a bandwidth of 7.2 GHz (336.6-343.8 GHz) is reported, where a range resolution of ~2.5 cm is achieved [9]. However, the required multiple stages of signal processing, such as frequency conversion, filtering and amplification, would not only increase the system complexity and cost, but also deteriorate the signal quality and the imaging performance. Recently, microwave photonic technologies have been proposed as a promising solution for generation and processing of high-frequency RF signals [10–13]. Many schemes for photonic generation of broadband LFM signals have been demonstrated [14–17], where a signal bandwidth over 10 GHz can be easily achieved. However, simple and convenient processing of such broadband signals without sacrificing signal fidelity is difficult. In a previously-reported photonics-based fully digital coherent radar [18], the potential of photonic technologies in future radar applications is demonstrated, but the signal bandwidth is only tens of MHz and signal processing in the sampling receiver

Optics EXPRESS

still restricts the operation frequency and bandwidth. To down-convert the high-frequency RF signals, many microwave photonic frequency conversion techniques have been proposed [19–21], but it is hard for a traditional radar receiver to process the down-converted baseband or intermediate frequency (IF)-band signals when a very large operation bandwidth is adopted.

In this paper, we propose and experimentally demonstrate a novel photonics-based radar to perform real-time and high-resolution ISAR imaging. In the transmitter, a broadband LFMCW signal is generated by frequency quadrupling of a low-speed electrical signal at a single integrated electro-optical modulator. In the receiver, the received LFMCW signal is de-chirped to a low-frequency signal based on phase modulation of a reference optical signal followed by optical filtering. This photonic de-chirp technique can directly process high-frequency and large bandwidth signals without frequency conversion, and the de-chirped signal can be sampled by a low-speed analog-to-digital converter (ADC) and processed in real time. High-resolution and real-time ISAR imaging can thus be achieved. One such photonics-based imaging radar at K band with an instantaneous bandwidth of 8 GHz is established. A recorded two-dimensional imaging resolution of ~2cm × ~2 cm is achieved, and the real-time imaging capability is verified. To the best of our knowledge, this is the first experimental demonstration of high-resolution and real-time ISAR imaging at centimeter-wave band.

2. Principle

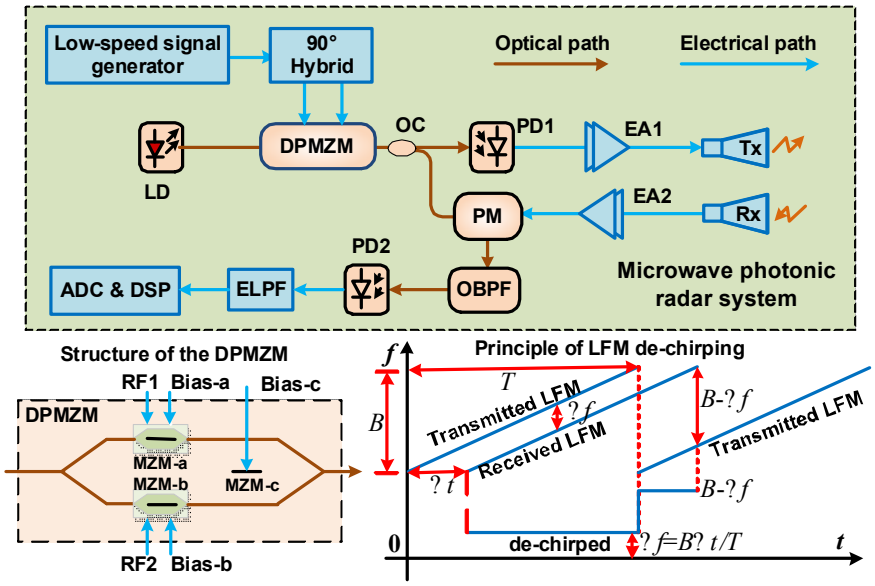

Fig. 1. Schematic diagram of the proposed photonics-based radar. LD: laser diode; OC: optical coupler; DPMZM: dual-parallel Mach-Zehnder modulator; PD: photodetector; EA: electrical amplifier; PM: phase modulator; OBPF: optical band-pased filter; ELPF: electrical low-pass filter; ADC: analog-to-digital converter; DSP: digital signal processing. The detailed structure of the DPMZM and the principle of the de-chirping are also provided.

Figure 1 shows the schematic diagram of the proposed photonics-based broadband radar. A continuous-wave (CW) light from a laser diode (LD) is modulated by a dual-parallel Mach-Zehnder modulator (DPMZM), which is driven by an IF-band LFMCW signal generated by a low-speed electrical signal generator. The instantaneous frequency of the IF-LFMCW signal can be expressed as $f_{IF}(t) = f_0 + kt$, where f_0 is the initial frequency and k is the chirp rate. The DPMZM consists of three sub-MZMs, where two sub-MZMs (MZM-a or MZM-b) are embedded in each arm of the main modulator (MZM-c), as shown in Fig. 1. Before applied to the DPMZM, the IF-LFMCW signal passes through an electrical 90° hybrid, which produces

Optics EXPRESS

two signals with 90° phase difference. The two signals are then fed to the RF ports of the two sub-MZMs. By biasing the two sub-MZMs at the maximum transmission points, a serial of even-order optical sidebands are generated. If the amplitudes of the driving signals are also properly controlled, only the optical carrier and the ± 2nd-order sidebands dominate, since the higher sidebands have very small amplitudes. Meanwhile, MZM-c is biased at the minimum transmission point to suppress the optical carrier. At the output of the DPMZM, only the ± 2nd-order optical sidebands exist [22], and the obtained optical signal can be expressed as

$$E_{\mathrm{DPMZM}}(t) \propto J_2(m)\cos\left[2\pi(f_c + 2f_{\mathrm{IF}})t\right] + J_2(m)\cos\left[2\pi(f_c - 2f_{\mathrm{IF}})t\right] \quad (1)$$

where f_c is the frequency of the LD, m is the modulation index of the two sub-MZMs, and J_2 denotes the 2nd-order Bessel function of the first kind. This optical signal is equally split into two branches by an optical coupler (OC). In the lower branch, the signal is used as a reference for de-chirp processing of the received radar echoes. In the upper branch, the optical signal is sent to a photodetector (PD1) to perform optical-to-electrical conversion. After PD1, a frequency-quadrupled LFMCW signal is obtained which has an instantaneous frequency of $f_{\mathrm{LFMCW}}(t) = 4f_0 + 4kt$. Compared with the input IF-LFMCW signal, both the center frequency and bandwidth of the generated LFMCW signal are quadruped. Based on this principle, broadband LFMCW signals can be easily generated using low-speed electrical devices.

The generated LFMCW signal is amplified by a broadband electrical amplifier (EA1) and emit to the free space through a transmit antenna for targets detection. The echoes reflected from the targets are collected by a receive antenna, which are properly amplified by another electrical amplifier (EA2) before applied to an electro-optical phase modulator (PM) to modulate the reference optical signal from the DPMZM. Mathematically, the reference optical signal can be treated as two optical carriers at f_c-$2f_0$-$2kt$ and $f_c + 2f_0 + 2kt$, which are both phase modulated by the reflected LFMCW signal. The frequency of the 1st-order sideband generated by phase modulating the carrier at f_c-$2f_0$-$2kt$ is located at $f_c + 2f_0 + 2kt + 4k\Delta\tau$, where $\Delta\tau$ is the time delay of the reflected LFMCW signal compared with the transmitted signal. By properly designing the parameters of the transmitted signal according to the detection range to let $4k\Delta\tau$ be a small value, this 1st-order sideband is very close to the optical carrier at $f_c + 2f_0 + 2kt$, so they can be extracted using an optical bandpass filter (OBPF). The optical signal after the OBPF is written as

$$E_{\mathrm{OBPF}}(t) \propto J_0(m')\cos\left[2\pi(f_c + 2f_0 + 2kt)t\right] + J_1(m')\cos\left[2\pi(f_c + 2f_0 + 2kt + 4k\Delta\tau)t + \frac{\pi}{2}\right] \quad (2)$$

where m' is the phase modulation index. After the OBPF, the optical signal is sent to another photodetector (PD2) to perform optical-to-electrical conversion. To this point, photonic de-chirping is implemented. The desired signal after de-chirping has a low frequency at $\Delta f = 4k\Delta\tau$, as illustrated in Fig. 1, where B is the bandwidth and T is the temporal period of the LFMCW signal. It should be noted that a high frequency component at B-Δf is generated at the same time, because of the temporal overlap between the received echo and the transmitted LFMCW signal in the next period. To remove the high frequency interference, an electrical low-pass filter (ELPF) with a proper bandwidth is applied after the PD. Since the frequency of the de-chirped signal after the ELPF is determined by the time delay ($\Delta\tau$) and chirp rate ($4k$) of the echo LFMCW signal, the distance of the target from the antenna pair can be calculated by

$$L = \frac{c}{2}\Delta\tau = \frac{c}{2}\cdot\frac{\Delta f}{4k} = \frac{cT}{2B}\Delta f \quad (3)$$

where c is the velocity of light in vacuum. For a moving target, an ISAR imaging can be constructed based on the principles provided in [4]. By choosing a proper chirp rate of the transmitted LFMCW signal according to the detection range, the de-chirped signal can be

Optics EXPRESS

controlled to have a low frequency (e. g., lower than 50 MHz), and it can be digitized by a low-speed ADC with a high effective number of bits. Then, the digitized signal can be processed in a digital signal processing (DSP) unit based on mature ISAR imaging algorithms. Supposing the de-chirped signal has M pulses in one frame and each pulse has N samples, the total samples make an $M \times N$ matrix. One-dimensional range profile is derived by performing N-point discrete Fourier transform (DFT) for all the M rows. After motion compensation, M-point inverse discrete Fourier transform (IDFT) is calculated in the cross range profile and a two-dimension image can be constructed [5]. When performing DFT in each row, the spectral resolution is the inverse of the measurement time [7], i.e., the minimum distinguishable spectral spacing is $\Delta f_{\min} = 1/T$. Thus, the theoretical range resolution of the radar is

$$L_{\mathrm{RES}} = \frac{cT}{2B}\Delta f_{\min} = \frac{c}{2B} \tag{4}$$

and the cross range resolution is given by [4]

$$C_{\mathrm{RES}} = \frac{c}{2\theta f_{\mathrm{c1}}} \tag{5}$$

where f_{c1} is the center frequency of the LFMCW signal, θ is the total viewing angle of target rotating.

According to (4), a large signal bandwidth helps to achieve a high range resolution. The proposed radar can avoid the use of multi-stage electrical frequency conversion as well as the high-speed ADCs, so it enables the generation and processing of broadband radar signals. In principle, the operation bandwidth is mainly limited by the electro-optical devices, which can reach tens or even hundreds of gigahertz. Thus, it is possible to achieve an ultra-high range resolution below 1 cm. The cross range resolution, which is determined by f_{c1} and θ, can be chosen to be the same as or close to the range resolution. Besides, processing of the de-chirped low frequency signal makes the system competent for very fast ISAR imaging using mature digital radar receivers. Therefore, the proposed photonics-based radar has the potential for ultra-high resolution and real-time imaging.

3. Experiment

To investigate the performance of the proposed photonics-based radar, a K-band radar with a bandwidth as large as 8 GHz is established based on the setup in Fig. 1. In the established system, an LD (TeraXion Inc.) with an output power of 18.0 dBm at 1550.12 nm is used as the light source. The CW light is modulated by a DPMZM (Fujitsu FTM7962EP), which has a 3-dB bandwidth of 22 GHz and a half-wave voltage of 3.5 V at 22 GHz. An LFMCW signal centered at 5.5 GHz with a bandwidth of 2 GHz (4.5-6.5 GHz) and a repetition rate of 200 kHz is generated by an arbitrary waveform generator (Keysight 8195A), which is used as the input electrical IF-LFMCW signal. After properly setting the bias voltages of the DPMZM, frequency quadrupling of the input IF-LFMCW signal is realized. Figure 2(a) shows the optical spectrum of the signal after the DPMZM, which is measured by an optical spectrum analyzer (Yokogawa AQ6370C) with a resolution of 0.02 nm. As shown in Fig. 2(a), two frequency-swept ± 2nd-order optical sidebands are generated with the undesired sidebands well suppressed. Following the DPMZM, a 50:50 OC is used to split the optical signal. The optical signal from one output port of the OC is sent to a 40-GHz PD (u2t XPDV2120RA). The waveform of the generated LFMCW signal in one period (5μs) is observed by an 80-GSa/s real-time oscilloscope (Keysight DSO-X 92504A), as shown in Fig. 2(b). Figure 2(c) shows the instantaneous frequency of the LFMCW signal recovered by short-time Fourier transform (STFT) analysis. As can be seen, the frequency is in the range from 18 to 26 GHz and the signal bandwidth is 8 GHz, confirming the successful frequency quadrupling.

Optics EXPRESS

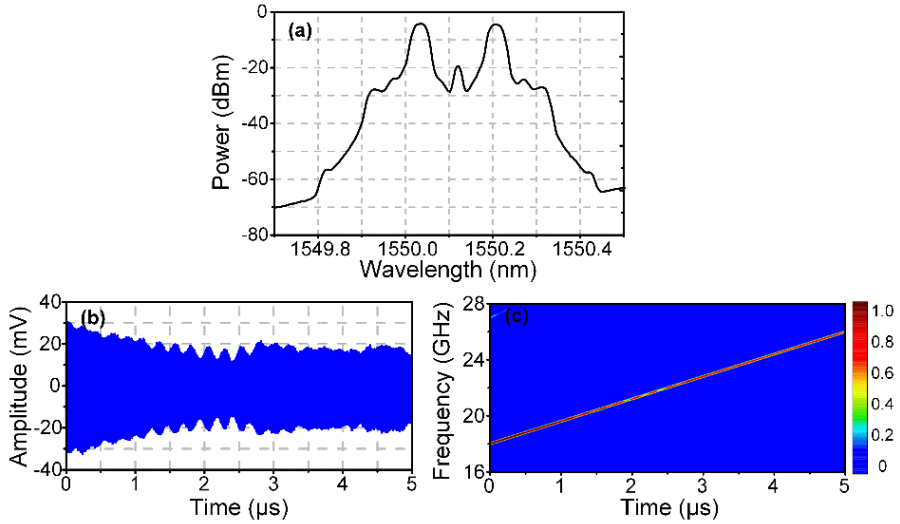

Fig. 2. Generation of an LFMCW signal with an 8-GHz bandwidth and a 5-μs period. (a) The measured optical spectrum after the DPMZM, (b) the temporal waveform and (c) the recovered instantaneous frequency of the generated LFMCW signal.

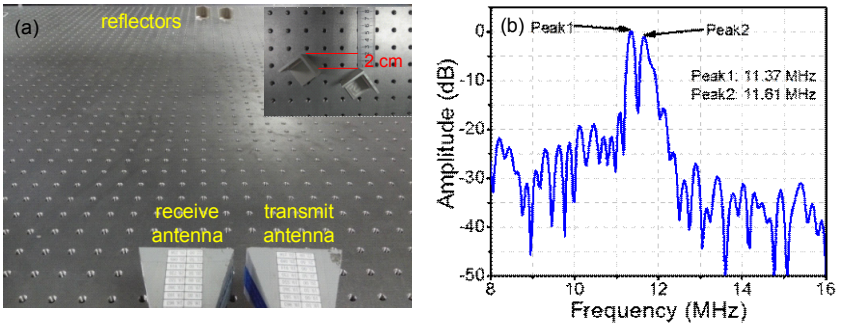

Fig. 3. (a) Configuration for detecting two trihedral corner reflectors which are separated by 2 cm along the radar line of sight, (b) spectrum of the de-chirped signal.

The generated LFMCW signal is amplified by a 40-GHz broadband electrical amplifier (SHF 806E) with a gain of 26 dB, and then sent to a K-band horn antenna for air transmission toward the targets. The echo signal is collected by another K-band horn antenna placed close to the transmit antenna. After being amplified by another broadband electrical amplifier (SHF 806E), the echo signal is sent to the RF port of a 40 GHz PM (EOSPACE Inc.). A narrow band tunable OBPF (Yenista XTM-50) is followed to select the required frequency components in Eq. (2). A 10-GHz PD (CONQUER Inc.) is used following the OBPF. To avoid the high frequency interference, the obtained electrical signal after the PD passes through an ELPF with a 3-dB bandwidth of 95 MHz. To check the range resolution of the radar system, two static small trihedral corner reflectors are placed at a distance of ~1 m away from the antenna pair, as shown in Fig. 3(a). Along the radar line of sight, the corners of the two reflectors are separated by 2 cm. The de-chirped signal is sampled and recorded by the real-time oscilloscope working at a sampling rate of 100 MSa/s. Figure 3(b) shows the spectrum obtained by performing fast Fourier transform (FFT) to the digital samples in one period (5μs) of the de-chirped signal. As can be seen, there are two clearly separated spectral peaks located at 11.37 MHz and 11.61 MHz, respectively. Based on Eq. (3), the distance

between two targets is proportional to the frequency spacing between the two spectral peaks after de-chirping. In this case, the distance between the two reflectors in the range profile is calculated to be 2.2 cm, which is close to the real value, indicating that the effective resolution to distinguish two targets in the range profile is better than 2.0 cm. According to (4), the theoretical range resolution of the 8-GHz bandwidth radar is as high as 1.875cm.

Then, ISAR imaging experiments are conducted. First, the targets are three silver-paper-packed balls with a diameter of 2.5 cm placed at the three vertexes of an equilateral triangle with 20-cm length of each side, as shown in Fig. 4(a). The equilateral triangle is centered at the rotating axis of a turntable, which is 2.65 m away from the radar antenna pair. In the experiment, the turntable is rotating in the horizontal plane with an angular speed of 2 degree per millisecond, and the antenna pair has a depression angle of about 10 degree towards the turntable rotating plane. The de-chirped signal is located at around 29 MHz. The signal in a duration of 10 ms is a sampled with a sampling rate of 100 MSa/s. The obtained digital signal consists of 2000 pulses with each pulse having 500 samples. Figure 4(b) shows the obtained ISAR image, where the three balls are clearly separated with a distance of ~20 cm between each other, which matches well with the real setup. The central spot in Fig. 4(b) is caused by the reflection from the metal area of the turntable axis. According to (5), the cross range resolution is determined by the center frequency of the LFMCW signal and the rotating angle of the target, which is 1.954 cm in this demonstration. Therefore, a two-dimensional imaging resolution as high as ~2cm × ~2cm is achieved.

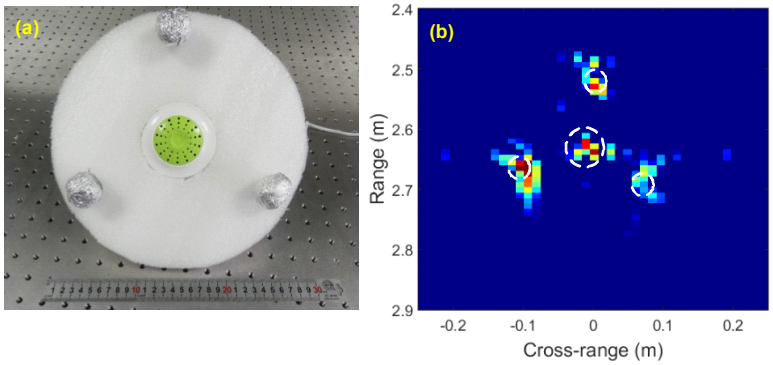

Fig. 4. (a) The photograph of three small balls under test, (b) Imaging result of the three small balls packed with silver paper.

To further evaluate the performance of the established radar, ISAR imaging of a small electric fan with its five blades packed with silver papers is performed. Figure 5(a) shows the picture of the electric fan when at rest. The length and width of each blade is 16 cm and 6 cm, respectively, and the distance between the turntable and the radar antenna pair is 2.35 m. The turntable is also rotating in the horizontal plane with an angular speed of 2 degree per millisecond. The de-chirped signal is at about 26 MHz, and it is also sampled at 100 MSa/s. The digital samples in a duration of 100 ms is recorded, of which the signal in every 10 ms is processed as a frame. Figure 5(b) shows the imaging result of the first frame. As can be seen, the five blades and the metal axis can be easily distinguished. Figure 5(c) and (d) shows the imaging results corresponding to the second frame and the fifth frame, respectively, in which high-resolution images are also achieved. The video in Visualization 1 shows the total 10 frames with a playback rate of 3 fps. It should be noted that, real-time digital signal processing at 100 MSa/s sampling rate is not a problem in modern digital radar receivers for constructing an ISAR image. Thus, fast ISAR imaging with a frame rate of 100 fps can be realized based on the established radar. If the radar applies an LFMCW signal with a lower chirp rate, which can be realized by adjusting the bandwidth and repetition rate of input IF-

Optics EXPRESS

LFMCW signal, the frequency of the de-chirped signal can be further reduced. Thus, the requirement for real-time imaging is also relaxed.

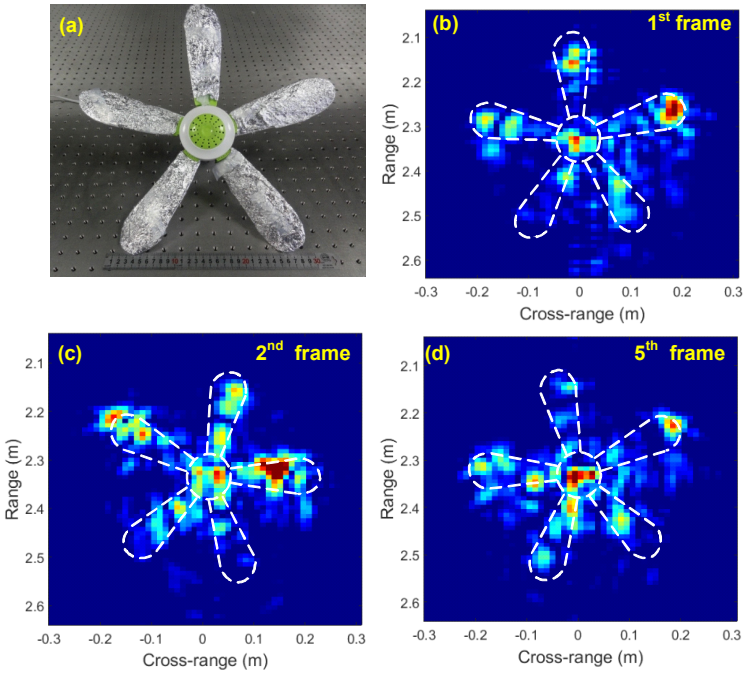

Fig. 5. (a) Photograph of the electric fan with its five blades packed with silver papers, (b) (c) and (d) is the imaging result for the first, second and fifth frame, respectively. A video including the total 10 frames with a playback rate of 3 fps is given in Visualization 1.

4. Conclusion

We have proposed and demonstrated a broadband photonics-based radar which has the ability for high-resolution and real-time target imaging. The system applies optical signal generation and de-chirp processing within a compact configuration, which avoids the use of electrical frequency conversion and high-speed ADCs. The broad operation bandwidth ensures a very high imaging resolution, and the receiver based on optical de-chirping enables fast or even real-time ISAR imaging. A K-band photonics-based radar with an 8-GHz bandwidth is established. Fast ISAR imaging with a frame rate of 100 fps is verified, and the two-dimensional imaging resolution reaches ~2 cm × ~2 cm. The proposed radar might be a promising solution for future real-time high-resolution target imaging.

Funding

Natural National Science Foundation of China (NSFC) (61401201, 61422108); the NSFC Program of Jiangsu Province (BK20140822); the Aviation Science Foundation of China (2015ZC52024) and the open fund of Science and Technology on Monolithic Integrated Circuits and Modules Laboratory (20150C1404).